ELSEVIER

Optical Materials 18 (2002) 355–365

OPTICAL Materials

www.elsevier.com/locate/optmat

Temperature dependencies of excited states lifetimes and relaxation rates of 3–5 phonon (4–6 μm) transitions in the YAG, LuAG and YLF crystals doped with trivalent holmium, thulium, and erbium

Yu.V. Orlovskii [a,*], T.T. Basiev [a], I.N. Vorob'ev [a], E.O. Orlovskaya [a], N.P. Barnes [b], S.B. Mirov [c]

[a] *Laser Materials and Technology Research Center of General Physics Institute RAS, 38 Vavilov st., Bld. D, 119991, GSP-1, Moscow, Russia*

[b] *NASA Langley Research Center, MS 474, Hampton, VA 23681, USA*

[c] *The University of Alabama at Birmingham, 1300 University Boulevard, Birmingham, AL 35294-1170, USA*

Received 9 April 2001; accepted 6 June 2001

Abstract

The temperature dependencies of the nanosecond multiphonon relaxation (MR) rates of the $^3F_3$ state of Tm^{3+} in the YLF crystal and of the $^5F_5$ state of Ho^{3+} ion in the YAG and LuAG crystals and of the microsecond MR rates of the $^4F_{9/2}$ ($^2H_{9/2}$) state of Er^{3+} ions in YLF were measured in the wide temperature range using direct laser excitation and selective fluorescence kinetics decay registration. For YLF the observed relations are explained by 4-phonon process in the frame of a single-frequency model with $h\omega_{\text{eff}} = 450 \pm 30$ cm^{-1} for the $^3F_3$ state of Tm^{3+} and by 5-phonon process with $h\omega_{\text{eff}} = 445$ cm^{-1} for the $^4F_{9/2}$ ($^2H_{9/2}$) state of Er^{3+}. For YAG and LuAG crystals these dependencies are explained by the 3-phonon process with $h\omega_{\text{eff}} = 630$ cm^{-1}. The decrease of the relaxation rate with the temperature in the range from 13 to 80 K was observed for the $^4F_{9/2}$ ($^2H_{9/2}$) state of Er^{3+} in the YLF crystal. It is explained by the redistribution of excited electronic states population of erbium ions over the higher lying Stark levels with different MR probabilities. A good fit of experimental temperature dependence (including the dropping part of the experimental curve) was obtained for single-frequency model ($h\omega_{\text{eff}} = 450$ cm^{-1}) with $W_{01} = 8.0 \times 10^4$ s^{-1} and $W_{02} = 4.7 \times 10^4$ s^{-1} accounting Boltzmann distribution of population over two excited Stark levels of the excited state of erbium ions. Employment of this model improves the fit between the experiment and the theory for the $^5F_5$ state of Ho^{3+} ion in YAG as well. Strong influence of the parameters of the non-linear theory of MR, i.e. the reduced matrix elements $U^{(k)}$ of electronic transitions and the phonon factor of crystal matrix η on the spontaneous MR rates was observed experimentally. The smaller these parameters the slower the spontaneous MR W_0. This fact can be used for searching new active crystal laser media for the mid-IR generation.

PACS: 78.50.−w; 71.70Ch

Keywords: Laser crystals; Rare-earth ions; Lifetimes; Multiphonon relaxation; Mid-IR transitions; Temperature dependence

* Corresponding author. Tel.: +7-095-1328376; fax: +7-095-135-0270.
E-mail address: orlovski@lst.gpi.ru (Y.V. Orlovskii).

0925-3467/02/$ - see front matter
PII: S0925-3467(01)00174-4

1. Introduction

Multiphonon relaxation (MR) rates were measured as a function of temperature for Ho, Er, and Tm in YAG, YLF, and LuAG and fit to a model that takes into account both the phonon energy and the level-to-level transition rates. In many approaches to this problem, the number of phonons required for non-radiative transition is assumed equal to the minimum number of phonons ($n_{\min}$) required to span the energy gap between manifolds. However, here it was found that the closest spaced levels with minimum number of phonons bridged the energy gap may not have sufficiently large transition rates because, for example, of the low density of phonon states close to the maximum energy phonon of a crystal. As a result, the transition with increased phonon number ($n_{\min}+1$) gives larger contribution to the overall MR rate due, for example, to higher density of effective phonon states than those for the maximum phonon. Also, another pair of levels in the manifolds that also require more phonons than $n_{\min}$ to relax may decrease the overall MR rate with the temperature increase due to smaller level-to-level transition rate. MR in rare-earth doped optical crystals was first studied in details in [1–4] based on semi-empirical model. Super-weak electron–phonon coupling model was later developed in [5–7].

This work is the continuation of our investigation of the MR regularities in the rare-earth doped laser crystals started in [8]. Since then more than forty 1–5 phonon transitions were directly measured and analyzed in the YAG, CGGG, GGG, $YAlO_3$, Y_2O_3, $CaMoO_4$, YLF, LaF_3, $Na_{0.4}Y_{0.6}F_{2.2}$, KY_3F_{10}, CaF_2 and SrF_2 crystals doped with Nd^{3+}; in YLF and LaF_3 doped with Er^{3+}, in YLF, YAG and LuAG doped with Ho^{3+}, and in YLF, YAG and LuAG doped with Tm^{3+} [8–14,16–18,20]. The regularities of MR rates depend on: the number of phonons n, the structure of crystal matrix, its lattice parameters, the type of cations and anions of the lattice, the type of optical center, the Stark splitting of the excited states of rare-earth ions, and the type of rare-earth ion (its ionic radius), on the type of electronic transition (on the values of its reduced matrix elements $U^{(k)}$ were found). They were explained [13,15, 16,19] in the frame of the non-linear mechanism of the theory of MR in the single-frequency approximation of crystal lattice vibrations developed in [5–7,13,15,16,19,21]. This mechanism accounts both point–charge and exchange–charge interaction between rare-earth ions and the ligands [5–7]. Exponential dependence of MR rates versus phonon number was established at $T = 0$ K:

$$W\ (T = 0\ \mathrm{K}) = W_0 = W\eta^n, \tag{1}$$

where W is the electronic and η is the phonon factor of the lattice in the single-frequency approximation. For further examination of the non-linear theory of MR it is interesting to measure temperature dependencies of the rates for different multiphonon transitions in rare-earth doped crystals. Such information is also very useful for the analysis of new laser materials for laser generation in the rare-earth doped oxide and fluoride laser crystals, specifically in the mid-IR spectral region.

2. Experimental details, results and discussion

2.1. The $^3F_3$ state of the Tm^{3+} ion in the YLF crystal

2.1.1. Experimental details

The $^3F_3$ state of the $LiYF_4$:Tm^{3+} (1%) crystal was excited through the $^3F_2$ state which is separated from the lower lying $^3F_3$ state by the small energy gap of $\Delta E \approx 500$ cm^{-1} (Fig. 1(a)). A pulsed tunable Oksazin-17 dye laser ($t_p \approx 5$ ns, $\lambda_{gen} =$ 632–670 nm) pumped with copper vapor laser ($t_p = 10$ ns, $f = 10$ kHz) excited the laser materials ($\lambda_{ex} = 657.1$ nm). Because the MR rate is so high, only a small fraction of the excited atoms relax by spontaneous emission. To compensate for the low fluorescent emission, a time-correlated photon-counting registration technique was used. It consisted of a MCA Trump-Plus PC Plug in Card; EG&G Ortec, EG&G NIM Electronics; PMT-79 with S-20 photocathode; and a MDR-23 monochromator with spectral resolution 13 Å/mm). The monochromator was set at the registration wavelength, $\lambda_{reg} = 688.2$ nm. The signal was recorded with time resolution less than 0.5 ns.

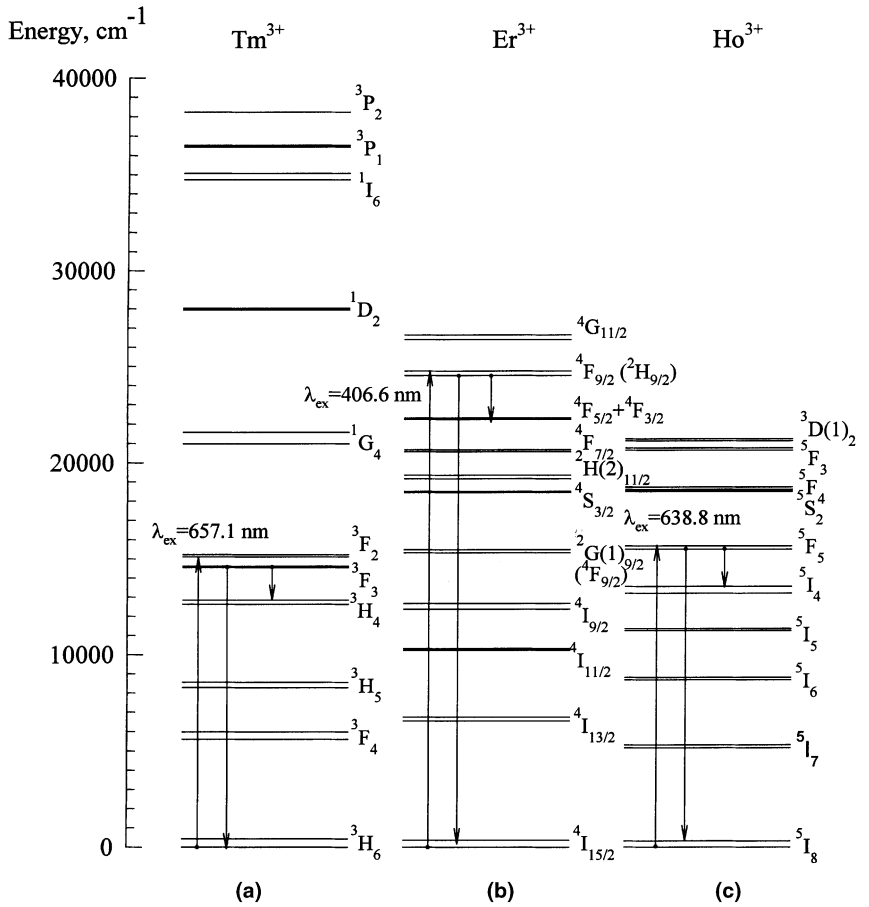

Fig. 1. The energy level diagram of rare-earth ions manifolds classified in the intermediate coupling approximation in: (a) YLF:Tm^{3+}; YLF:Er^{3+}; and (c) YAG:Ho^{3+}. For two manifolds of erbium the notation in the LS-coupling approximation is given in brackets.

2.1.2. Results and discussion

The measured temperature dependence of the short initial stage decay of the $^3F_3$ state of Tm^{3+} in YLF is presented in Table 1. The contribution of the radiative relaxation was negligible ($A = 1940\ s^{-1}$). The MR rate W_{MR} was calculated using equation $W_{MR} = 1/\tau_{meas} - A$, where $A = 1940\ s^{-1}$ is the radiative probability calculated using Judd–Ofelt theory. Intensity parameters Ω_k were taken from [22]. The excited-state notations determined in the intermediate coupling approximation rather than LS-coupling, the reduced matrix elements of electro-dipole transitions $U^{(k)}$ and thulium magnetic-dipole operators M were taken from [23]. Single-exponential kinetics decay with $\tau = 78$ ns was measured at $T = 77$ K [16,17]. At $T = 295$ and $T = 343$ K a non-exponential decay was observed. To determine the reason of this, the

Table 1
The temperature dependence of the lifetime of the $^3F_3$ state in the YLF:Tm^{3+} crystal

T, K	τ, ns	T, K	τ, ns	T, K	τ, ns
77	78 ± 1	343	$41 \pm 1/88.1$	473	27 ± 1
295	$54 \pm 1/595 \pm 5$	423	36 ± 1	–	–

dependence of kinetics decay versus fluorescence excitation (λ_{ex}) and registration (λ_{reg}) wavelengths were measured. The curve fitting with two exponential functions with different decay times τ_1 and τ_2 was done. In Table 1 and thereafter the non-exponential nature is marked by a slash between the lifetimes of initial and final stages. The first exponential component of the curve at $T = 295$ K does not depend on the excitation and registration wavelength ($\tau = 54$ ns). On the other hand, for the second exponential component different decay times were obtained (from 580 to 610 ns). However, the accuracy of determination of the latter ones was very poor. The same is true for $T = 343$ K. At $T = 423$ K ($\tau = 36$ ns) and $T = 473$ K ($\tau = 27$ ns) the single-exponential kinetics decay was observed.

The temperature dependencies of MR rate from the $^3F_3$ state of YLF:Tm was analyzed in the single-frequency model. In this simple model [4] theoretical dependencies were calculated in accordance with the following equations:

$$W_{MR}(T) = W\ (T = 0\ \mathrm{K})\ (n(\omega, T) + 1)^n, \tag{2}$$

$$n(\omega, T) = (\exp(h\omega_{eff}/kT) - 1)^{-1}, \tag{3}$$

where n is the number of phonons involved in the process; $n(\omega, T)$ is the population of a phonon mode of frequency ω at a temperature T described by the Bose–Einstein distribution. The experimental points for W_{MR} in the temperature range from 77 to 473 K are presented in Fig. 2. Also the theoretical curves indicate the expected temperature dependencies for fixed numbers of phonons $n = 3$, 4 and 5 when the energy "gap" ΔE between $^3F_3$ and $^3H_4$ was varied between $\Delta E_{min} = 1700\ \mathrm{cm}^{-1}$ and $\Delta E_{max} = 1996\ \mathrm{cm}^{-1}$. The variation in this energy gap due to Stark splitting. In the frame of this model 3-phonon process can be possible only between the lowest Stark level of $^3F_3$ and highest Stark level of $^3H_4$ that is for $\Delta E_{min} = 1700\ \mathrm{cm}^{-1}$ with maximum phonon frequency $h\omega_{eff} = 570\ \mathrm{cm}^{-1}$ for YLF crystal. But it is seen that both 3-phonon and the 5-phonon processes (see Fig. 2, curves 1, 4 and 5) fail to describe the experimentally measured temperature dependence. The theoretical curves which has been drawn in for

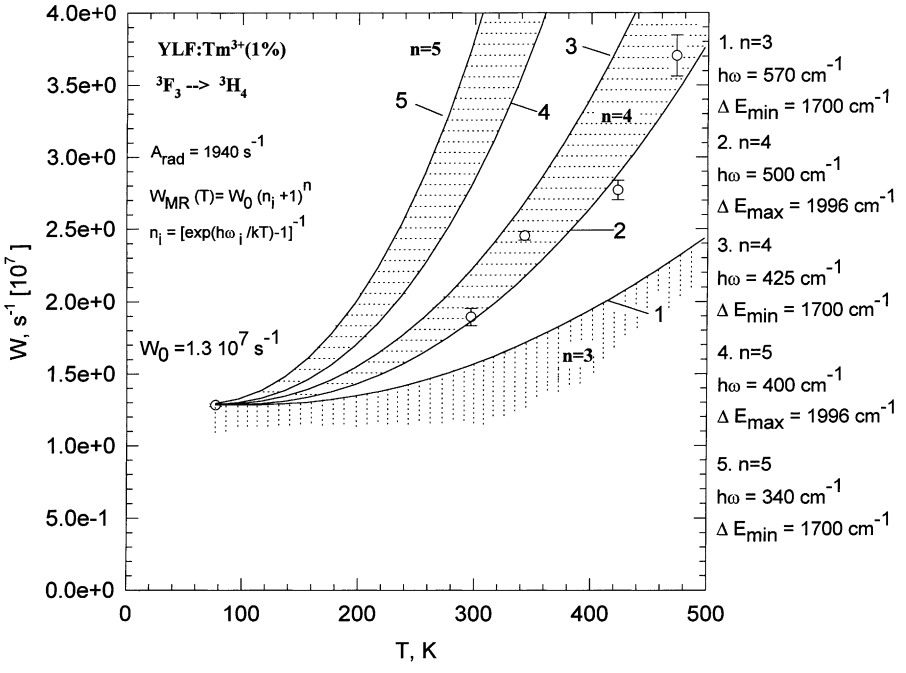

Fig. 2. Temperature dependence of experimental rates for the $^3F_3$ state in the YLF:Tm^{3+} crystal and the fitting curves for the single-frequency model.

the temperature stimulated emission by 4-phonon processes ($h\omega_1 = \Delta E_{min}/4 = 425$ cm^{-1}, curve 3 in Fig. 2 and $h\omega_2 = \Delta E_{max}/4 = 500$ cm^{-1}, curve 2 in Fig. 2) depict the boundaries of the area which covers all experimental points. Thus, the single-frequency model describes well the whole measured temperature dependence of relaxation by 4-phonon process with $h\omega_{eff} \cong (h\omega_1 + h\omega_2)/2 = 450 \pm 30$ cm^{-1}. The value of effective phonon obtained coincides well with the value of effective phonon $h\omega_{eff} = 480 \pm 20$ cm^{-1}, which stimulates $^4G_{7/2} \rightarrow {}^4G_{5/2}$ 3-phonon transition in the YLF:Nd^{3+} crystal with the temperature increase [14]. Also, this result is in agreement with the Raman spectra of the $LiYF_4$ crystal lattice, which was studied recently in [24,25].

2.2. The $^4F_{9/2}$ ($^2H_{9/2}$) state of the Er^{3+} ion in the YLF crystal

2.2.1. Experimental details

For direct measurements of kinetics of fluorescence decay of the $^4F_{9/2}$ ($^2H_{9/2}$) state (Fig. 1(b)) in YLF:Er^{3+} (0.4%) crystal at T less or equal 270 K the LiF:F_2^+ color center laser ($t_p = 50$ ns, $\lambda_{gen} =$ 810–1210 nm) pumped by Alexandrite laser ($f = 20$ Hz, $t_p = 70$ ns, $\lambda_{gen} = 720$–760 nm) was used. The 25° cut BBO non-linear crystal was used for type I SHG. The fluorescence was registered at 412.8 nm. For $T > 270$ K 398 nm excitation into anti-stokes phonon side-band was realized with a D_2 Raman cell pumped in a back scattering geometry by the third harmonics of YAG:Nd laser ($f = 10$ Hz, $t_p = 4$ ns). Fluorescence registration at 413.6 nm was done. For the fluorescence selection and registration ARC-750 spectrometer and R928 Hamamatsu PMT were used. Signal acquisition, recording and treatment was provided by Tektronix TDS-380 (350 MHz bandwidth) digital averaging oscilloscope. The closed-cycle Janis cryostat with temperature controller was used for YLF:Er^{3+} crystal cooling in the range from 13 to 270 K and heating from 300 to 475 K.

2.2.2. Results and discussion

The measured temperature dependence of the fluorescence kinetics decay lifetime of the $^4F_{9/2}$ ($^2H_{9/2}$) state of Er^{3+} in YLF is presented in Table 2. The experimental points for W_{MR} in the temperature range from 13 to 475 K are presented in Figs. 3 and 4. The MR rate W_{MR} was calculated using equation $W_{MR} = 1/\tau_{meas} - A$, where $A = 3340$ s^{-1} is the radiative probability calculated using Judd–Ofelt theory with intensity parameters Ω_k taken from [26]. Other parameters including magnetic dipole operators M for erbium transitions and manifolds notations in the intermediate coupling approximation were taken from [23]. Therefore, the manifold in study indicated previously by many authors as $^2H_{9/2}$ is classified now as

Table 2
The temperature dependence of the lifetime of the $^4F_{9/2}$ ($^2H_{9/2}$) state in the YLF:Er^{3+} crystal

T, K	τ, μs	T, K	τ, μs	T, K	τ, μs
13.6	12.4 ± 0.2	75.3	13.3 ± 0.2	220.1	10.5 ± 0.2
13.8	12.3 ± 0.1	80.4	13.5 ± 0.2	230.1	10.0 ± 0.20
14.3	12.6 ± 0.1	90.5	13.2 ± 0.2	240.4	9.6 ± 0.2
19.6	12.7 ± 0.2	101.4	13.1 ± 0.2	250.4	8.6 ± 0.2
20.5	12.7 ± 0.5	110.4	13.3 ± 0.2	260.3	8.9 ± 0.2
24.6	12.6 ± 0.2	120.4	13.2 ± 0.2	270.2	8.2 ± 0.2
29.3	12.7 ± 0.2	130.4	12.8 ± 0.2	297.3	7.6 ± 0.2
34.6	12.9 ± 0.3	140.4	12.3 ± 0.2	301.2	7.2 ± 0.1
40	12.7 ± 0.2	150.3	12.4 ± 0.2	326.0	6.9 ± 0.1
44.8	12.6 ± 0.2	160.4	12.1 ± 0.2	350.9	6.2 ± 0.1
49.9	13.1 ± 0.2	170.2	11.9 ± 0.2	375.8	5.5 ± 0.1
54.9	13.1 ± 0.2	180.3	11.5 ± 0.2	400.6	5.1 ± 0.1
60	13.4 ± 0.2	190.2	11.1 ± 0.2	425.2	4.4 ± 0.1
65	12.8 ± 0.2	200.2	10.6 ± 0.2	449.6	4.2 ± 0.1
70.3	13.2 ± 0.2	210.2	10.5 ± 0.2	474.5	3.8 ± 0.2

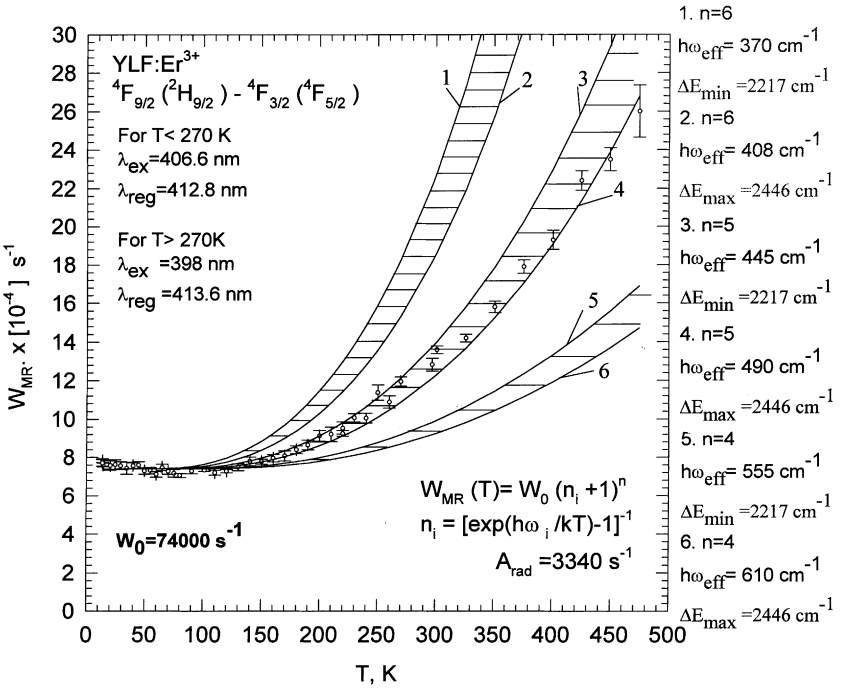

Fig. 3. Temperature dependence of experimental rates for the $^4F_{9/2}(^2H_{9/2})$ state in the YLF:Er^{3+} crystal and the fitting curves for the single-frequency model.

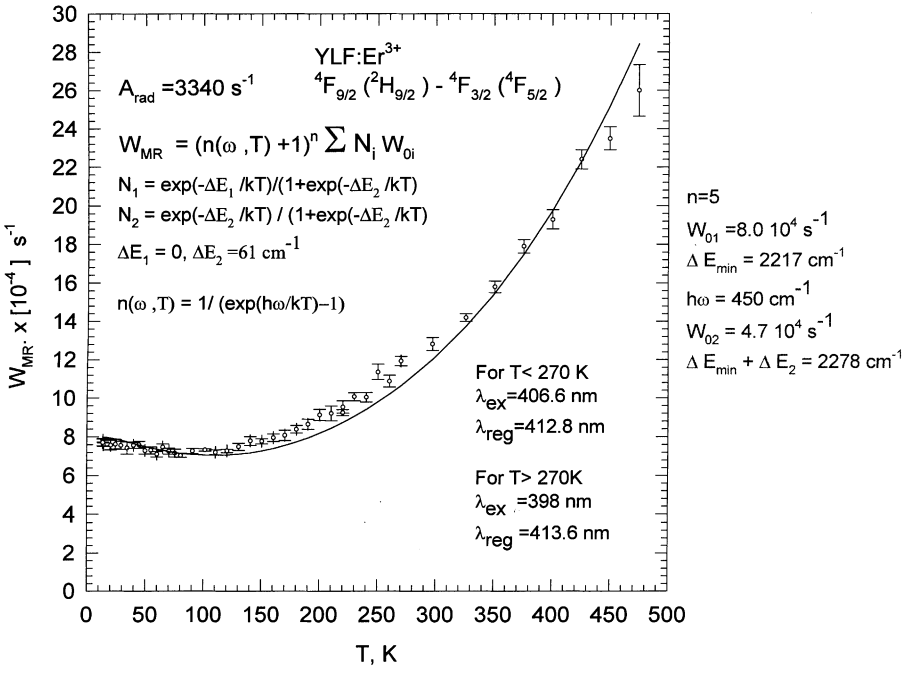

Fig. 4. Temperature dependence of experimental rates for the $^4F_{9/2}(^2H_{9/2})$ state in the YLF:Er^{3+} crystal and the fitting curves for the single-frequency model accounting Boltzmann distribution of population over two Stark levels of the excited state.

$^4F_{9/2}$. The temperature dependence of MR rate from the $^4F_{9/2}$ ($^2H_{9/2}$) state of YLF:Er^{3+} was analyzed in single-frequency approximation of phonon spectrum. (Fig. 3). The theoretical curves indicate the expected temperature dependencies for fixed numbers of phonons $n = 4$, 5 and 6 when the energy "gap" ΔE between the $^4F_{9/2}$ ($^2H_{9/2}$) and $^4F_{3/2}$; $^4F_{5/2}$ states is varied from $\Delta E_{min} = 2217$ to $\Delta E_{max} = 2446$ cm^{-1} due to Stark splitting of the $^4F_{9/2}$ ($^2H_{9/2}$) state with $W_0 = 7.4 \times 10^4$ s^{-1} calculated from the low temperature fit. The best fit in the frame of this model was obtained for the 5-phonon process ($n = 5$) with $h\omega_{eff} = \Delta E_{min}/5 = 445$ cm^{-1} (curve 3 of Fig. 3). As a result, the transition with increased phonon number ($n_{min} + 1$) gives larger contribution to the overall MR rate due, for example, to higher density of effective phonon states than those for the maximum phonon.

The decrease of the relaxation rate with the temperature in the range from 13 to 80 K can be explained by the redistribution of excited electronic states of erbium ions among the Stark levels with different MR probabilities. Fig. 4 presents the fit of experimental data using the following equations accounting Boltzmann distribution of population over the Stark levels of the excited state of erbium ions:

$$W_{MR}(T) = (n(\omega, T) + 1)^n \sum N_i W_{0i}, \quad (4)$$

where

$$N_i = \exp(-\Delta E_i/kT) / \sum \exp(-\Delta E_i/kT) \quad (5)$$

and

$$n(\omega, T) = (\exp(h\omega/kT) - 1)^{-1}. \quad (6)$$

A rather good fit was obtained accounting second Stark level of the $^4F_{9/2}$ ($^2H_{9/2}$) state, only, with energy gap $\Delta E_2 = 61$ cm^{-1} and single-frequency approximation with $h\omega_{eff} = 450 \pm 5$ cm^{-1}. Almost two times difference of the values of $W_{01} = 8.0 \times 10^4$ s^{-1} and $W_{02} = 4.7 \times 10^4$ s^{-1} was found. Hence, we see, that another pair of levels in the manifolds that also require more phonons than n_{min} to relax may decrease the overall MR rate with the temperature increase due to smaller level-to-level transition rate. The values of Stark splitting of the $^4F_{9/2}$ ($^2H_{9/2}$) state was taken from [27]. The value of the effective phonon obtained is in the range with the value of effective phonon found for the warm-up stimulation of the $^3F_3$–$^3H_4$ 4-phonon transition in the $LiYF_4$:Tm^{3+} (1%) crystal ($h\omega_{eff} = 450 \pm 30$ cm^{-1}). The very interesting result is that the probability of spontaneous multiphonon emission from different Stark levels might differ almost two times because of different intra – state Stark – to Stark squared matrix elements.

2.3. The $^5F_5$ state of the Ho^{3+} ion in YAG and LuAG crystals

2.3.1. Experimental details

For direct measurements of the kinetics of fluorescence decay of the $^5F_5$ state in YAG:Ho^{3+} and LuAG:Ho^{3+} (see Fig. 1(c)) the same laser source was used as for the excitation of the $^3F_3$ state of YLF:Tm^{3+}. As the result at $\lambda_{ex} = 638.8$ and $\lambda_{reg} = 670$ nm, the single-exponential kinetics decay with $\tau = 388$ ns in YAG:Ho^{3+} and $\tau = 348$ ns in LuAG:Ho^{3+} was measured at $T = 77$ K [16,17]. For $T = 295$ K the kinetics decay (with $\tau = 375$ ns in 0.1–2.0% YAG:Ho^{3+} and $\tau = 343$ ns in 0.1–1.0% LuAG:Ho^{3+}) does not depend on concentration of Ho^{3+} ions. For this reason the YAG:Ho^{3+} (2%) and LuAG:Ho^{3+} (1%) crystals were used for the temperature dependence measurements of the MR rates as the fluorescence signal was very weak for YAG:Ho^{3+} (0.1%) and LuAG:Ho^{3+} (0.1%) crystals at high temperatures. At $T = 773$ K the small non-exponential nature was observed in LuAG:Ho^{3+}, which obviously deals with the scattering of pump laser light.

2.3.2. Results and discussion

The measured temperature dependence of lifetime of the $^5F_5$ state of Ho^{3+} in YAG and LuAG is presented in Table 3. The contribution of the radiative relaxation to the measured lifetimes is negligible ($A = 5460$ and 4160 s^{-1} for YAG:Ho^{3+} and LuAG:Ho^{3+}, respectively). The radiative probabilities A were calculated using Judd–Ofelt theory with intensity parameters Ω_k taken from [28,29], respectively for YAG and LuAG, and other parameters including magnetic-dipole operators M for holmium were taken from [23].

Table 3
The temperature dependence of the lifetime of the $^5F_5$ state

T, K	τ, ns	T, K	τ, ns	T, K	τ, ns
(a) YAG:Ho^{3+} crystal					
77	388 ± 5	423	290 ± 8	603	220 ± 30
295	375 ± 5	473	265 ± 6	607	210 ± 15
333	353 ± 5	508	254 ± 8	653	172 ± 5
373	332 ± 5	553	224 ± 6	693	160 ± 15
(b) LuAG:Ho^{3+} crystal					
77	348 ± 3	473	225 ± 3	673	138 ± 1.5
295	343 ± 2	523	197 ± 1.5	723	124 ± 1.5
373	292 ± 6	573	175 ± 1.5	773	$29.4/115 \pm 5$
423	257 ± 2	623	155 ± 1.5	–	–

The temperature dependencies of MR rate (W_{MR}) from the $^5F_5$ state in the YAG:Ho^{3+} and LuAG:Ho^{3+} crystals were analyzed using a single-frequency model of phonon spectrum. Fig. 5 present the experimental points of W_{MR} for YAG:Ho^{3+} in the temperature range from 77 to 693 K. The theoretical curves indicate the expected temperature dependence for the emission of fixed numbers of phonons $n = 3$ and 4 when the energy "gap" ΔE between $^5F_5$ and $^5I_4$ is varied between $\Delta E_{min} = 1894$ cm^{-1} and $\Delta E_{max} = 2463$ cm^{-1} due to Stark splitting. The values of Stark splitting for the YAG:Ho^{3+} crystal [30] were used during this analysis for both YAG and LuAG crystals. Two phonons ($n = 2$) with maximum phonon frequency allowed for YAG ($h\omega_{eff} = 850$ cm^{-1}) does not bridge the minimal energy gap ΔE_{min}. A comparison of the experimental and theoretical dependencies shows that for both garnet crystals the fit is poor for 4-phonon processes. At the same time the temperature stimulation of multiphonon emission at low temperatures range from 77 to 400 K is described well by a model using a 3-phonon process with $W_0 = 2.5 \times 10^6$ s^{-1} for YAG and $W_0 = 2.87 \times 10^6$ s^{-1} for LuAG and with $h\omega_{eff} = 820$ cm^{-1} that is close to the maximum phonon frequency allowed (see curve 4 in Fig. 5 for YAG:Ho^{3+} and Fig. 6 for LuAG: Ho^{3+}). Whereas in the high temperature range of 400–800 K the 3-phonon process with lower $h\omega_{eff} = 630$ cm^{-1} and the same W_0 parameter will be more effective (see curve 3 in Figs. 5 and 6).

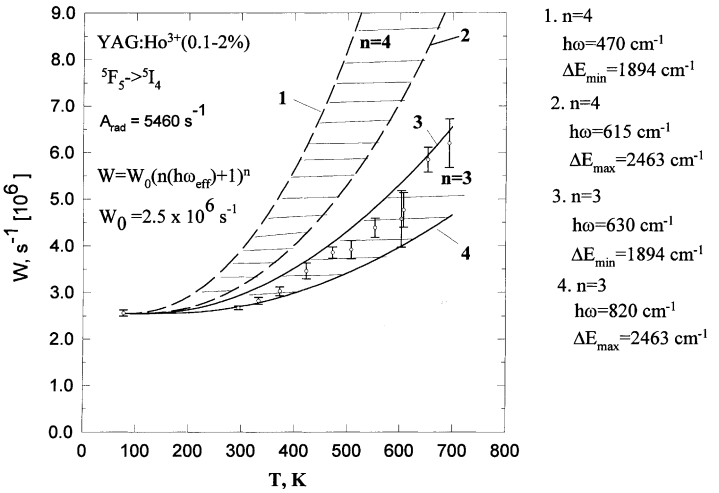

Fig. 5. Temperature dependence of experimental rates for the $^5F_5$ state in theYAG:Ho^{3+} crystal and the fitting curves for the single-frequency model.

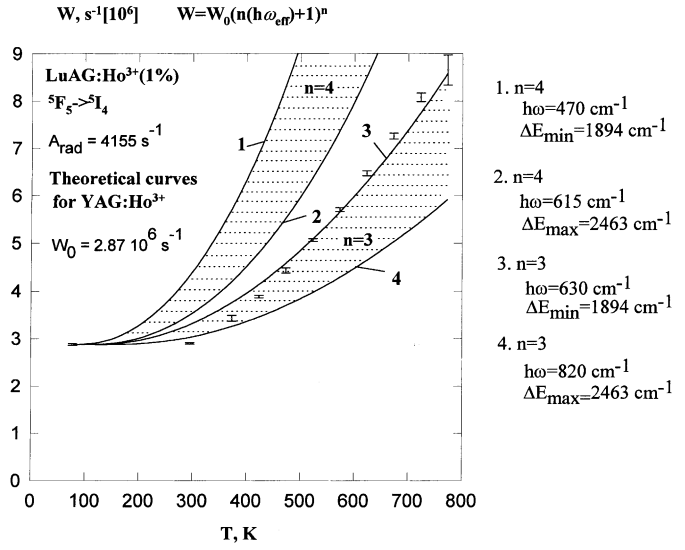

Fig. 6. Temperature dependence of experimental rates for the $^5F_5$ state in the LuAG:Ho^{3+} crystal and the fitting curves for the single-frequency model.

Normalization of the experimental MR rates dependence for YAG using the experimental points for the temperatures higher than 295 K with the help of single-frequency model for 3-phonon process with $h\omega_{\text{eff}} = 630\ \text{cm}^{-1}$ gives a good fit for all experimental points except for the low temperatures (curve 1 of Fig. 7). To have a better fit with the theory an approximation of the Stark splitting of the $^5F_5$ state of Ho^{3+} in YAG by two levels with $\Delta E = 56\ \text{cm}^{-1}$ was used. Same equations as for description of the $^4F_{9/2}$ ($^2H_{9/2}$) state MR rate temperature dependence in YLF:Er^{3+}

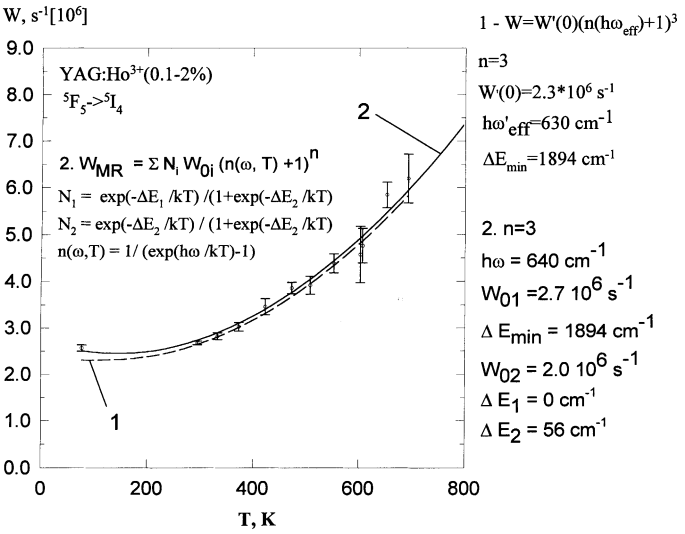

Fig. 7. Temperature dependence of experimental rates for the $^5F_5$ state in the YAG:Ho^{3+} crystal and the fitting curves for the single-frequency model: 1 – normalized to the experimental points at high temperatures; 2 – accounting Boltzmann distribution of population over two Stark levels of the excited state.

Table 4
Some parameters of optical transitions in laser crystals

Crystal	Transition	$U^{(2)}U^{(4)}U^{(6)}$	$A_{ed}+A_{md}$, s^{-1}	n, number of phonons	τ_{meas}, 77 K	W_0, s^{-1}
YAG:Ho	$^5F_5$–$^5I_4$	0.0001 0.0059 0.0004	5460	3	388 ns	2.6×10^6
YLF:Tm	$^3F_3$–$^3H_4$	0.081 0.344 0.264	1940	4	78 ns	1.3×10^7
YLF:Er	$^4F_{9/2}$–$^4F_{3/2}$	0.0134 0.0497 0.0141	3340	5	13.5 μs	7.4×10^4

were used. The energy gap ΔE is that between the lowest and highest Stark levels of the first group of Stark levels with close values of energies. As the result a very good fit between the theory and experiment was obtained for $n=3$ ($\hbar\omega_{eff}=640\ cm^{-1}$) with $W_{01}=2.7\times10^6\ s^{-1}$ and $W_{02}=2.0\times10^6\ s^{-1}$ (curve 2 of Fig. 7). The same procedure can be used for LuAG:Ho^{3+}. Unfortunately, right now we do not know the Stark splittings of the Ho^{3+} states in LuAG.

It is interesting to compare the obtained values of lifetimes for 3-phonon process in YAG:Ho^{3+} and 4-phonon process in YLF:Tm^{3+}. At a glance it seems strange that the lifetime is five times shorter for 4-phonon process when compared to a 3-phonon (see Table 4). But according to the nonlinear theory of MR this is not a strange result. The reduced matrix elements $U^{(k)}$ are 2–4 orders of magnitude larger for the 4-phonon transition and, therefore, the electronic factor W of Eq. (1) calculated in [16,17] is five orders larger for the 4-phonon process than for the 3-phonon one (10^{19} and $10^{14}\ s^{-1}$, respectively). Also, due to larger maximum phonon frequency in YAG ($\hbar\omega_{max}=850\ cm^{-1}$) comparing to YLF ($\hbar\omega_{max}=560\ cm^{-1}$) and larger minimal distance between rare-earth ion and the nearest ligands ($R_0=2.37$ Å) in YAG in comparison with YLF ($R_0=2.27$ Å) the phonon factor ($\eta\sim1/R_0^2\ 1/\hbar\omega_{max}$ [16]) is smaller in YAG. This gives additional reduction of the MR rate for the 3-phonon process in YAG:Ho^{3+}. If we compare 4- and 5-phonon transitions in YLF:Tm^{3+} and YLF:Er^{3+} with the same phonon factor η we observe more than two orders of magnitude decrease of the MR rate for the 5-phonon transition. This is in a qualitative agreement with the power law of Eq. (1). Also, the reduced matrix elements $U^{(k)}$ for 5-phonon transition in Er^{3+} are of one order of magnitude smaller than for 4-phonon transition in Tm^{3+}.

3. Conclusion

It was found that in first approximation a simple single-frequency model of crystal lattice vibrations can predict rather well the temperature dependencies of the MR rates of the $^3F_3$ state of Tm^{3+} and of the $^4F_{9/2}$ ($^2H_{9/2}$) state of Er^{3+} in YLF, and of the $^5F_5$ state of Ho^{3+} ion in YAG and LuAG. But some observed peculiarities, e.g. the decrease of MR rates for the $^4F_{9/2}$ ($^2H_{9/2}$)–$^4F_{3/2}$;$^4F_{5/2}$ erbium transition in YLF with the temperature increase in the range of 13–80 K could not be predicted in the frame of this simple model. Accounting of for the Boltzmann distribution of population over the Stark levels of the excited state and the difference of the MR rates from different Stark levels of the excited state explains very well the obtained temperature dependence in the single-frequency model. It was experimentally found that the probability of spontaneous multiphonon emission from different Stark levels might differ almost two times.

Strong influence of the parameters of the nonlinear theory of MR, i.e. the reduced matrix elements $U^{(k)}$ of electronic transitions and the phonon factor of crystal matrix η on the spontaneous MR transition rates W_0 is proved experi-

mentally. The smaller these parameters the slower the spontaneous MR. This fact can be used for searching new active crystal laser media for the mid-IR generation.

Acknowledgements

This work was partially supported by NASA Langley Research Center P.O. No. 47995D, RFBR grants 00-02-17108a and 99-02-18212a, INTAS 96-0232, NSF grant ECS- 9710428 and CRDF grant RE0- 825. We would like to thank B.Z. Malkin and K.K. Pukhov for helpful theoretical discussions.

References

[1] M.J. Weber, Phys. Rev. 156 (1967) 231.
[2] W.D. Partlow, H.W. Moos, Phys. Rev. 157 (1967) 252.
[3] M.J. Weber, Phys. Rev. 157 (1967) 262.
[4] L.A. Riseberg, H.W. Moos, Phys. Rev. 174 (1968) 429.
[5] K.K. Pukhov, V.P. Sakun, Phys. Stat. Sol. B 95 (1979) 391.
[6] K.K. Pukhov, Sov. Phys. Solid State 31 (1989) 1557.
[7] K.K. Pukhov, et al., Covalent non-linear mechanism of non-radiative relaxation of Ln^{3+} ions in crystals, Institute of Crystallography of Russian Academy of Sciences preprint N8, 1989, p. 1 (in Russian).
[8] T.T. Basiev, A.Yu. Dergachev, E.O. Kirpichenkova (Orlovskaya), Yu.V. Orlovskii, V.V. Osiko, Sov. J. Quantum Electron. 17 (10) (1987) 1289.
[9] T.T. Basiev, A.Yu. Dergachev, Yu.V. Orlovskii, Rev. Roum. Phys. 34 (1989) 789.
[10] T.T. Basiev, A.Yu. Dergachev, Yu.V. Orlovskii, in: M.L. Shand, H.P. Jenssen (Eds.), OSA Proceeding Series, Tunable Solid State Lasers, vol. 5, Optical Society of America, Washington, D.C., 1989, p. 130.
[11] T.T. Basiev, A.Yu. Dergachev, Yu.V. Orlovskii, A.M. Prokhorov, J. Lumin. 53 (1992) 19.
[12] T.T. Basiev, A.Yu. Dergachev, Yu.V. Orlovsky, V.V. Osiko, A.M. Prokhorov, Izv. Ross. Akad. Nauk, Ser. Fiz. 56 (1992) 113 (Russia).
[13] Yu.V. Orlovskii, R.J. Reeves, R.C. Powell, T.T. Basiev, K.K. Pukhov, Phys. Rev. B 49 (1994) 3821.
[14] T.T. Basiev, A.Yu. Dergachev, Yu.V. Orlovskii, A.M. Prokhorov, in: Proceedings of General Physics Institute, vol. 46, Nauka, Moscow, 1994, p. 3.
[15] Review: Yu.V. Orlovskii, K.K. Pukhov, T.T. Basiev, T. Tsuboi, Opt. Mater. 4 (1995) 583.
[16] T.T. Basiev, Yu.V. Orlovskii, K.K. Pukhov, V.B. Sigachev, M.E. Doroshenko, I.N. Vorob'ev, J. Lumin. 68 (1996) 241.
[17] T.T. Basiev, Yu.V. Orlovskii, K.K. Pukhov, V.B. Sigachev, M.E. Doroshenko, I.N. Vorob'ev, OSA Trends in Optics and Photonics (TOPS) Volume on Advanced Solid State Lasers, vol. 1, 1996, p. 575.
[18] Yu.V. Orlovskii, T.T. Basiev, I.N. Vorob'ev, V.V. Osiko, A.G. Papashvili, A.M. Prokhorov, Laser Phys. 6 (1996) 448.
[19] Review: T.T. Basiev, Yu.V. Orlovskii, K.K. Pukhov, F. Auzel, Laser Phys. 7 (1997) 1139.
[20] Yu.V. Orlovskii, T.T. Basiev, S.A. Abalakin, I.N. Vorob'ev, O.K. Alimov, A.G. Papashvili, K.K. Pukhov, J. Lumin. 76/77 (1998) 371.
[21] K.K. Pukhov, T.T. Basiev, Yu.V. Orlovskii, M. Glasbeek, J. Lumin. 76/77 (1998) 586.
[22] C. Li, Y. Guyot, C. Linares, R. Moncorge, M.F. Joubert, in: OSA Proceedings on Advanced Solid States Lasers, vol. 15, 1993, p. 91.
[23] A. Kornienko, unpublished.
[24] S. Salaun, M.T. Fornoni, A. Bulou, M. Rousseau, P. Simon, J.Y. Gesland, J. Phys. Condens. Matter 9 (1997) 6941.
[25] S. Salaun, A. Bulou, M. Rousseau, B. Hennion, J.Y. Gesland, J. Phys. Condens. Matter 9 (1997) 6957.
[26] G.J. Kintz, L. Esterowitz, R. Allen, Appl. Phys. Lett. 50 (1987) 1553.
[27] H.P. Christinsen, Phys. Rev. B 19 (1979) 6564.
[28] B.M. Antipenko, Yu.V. Tomashevich, Sov. J. Opt. Spectrosc. 44 (1978) 272.
[29] D.N. Patel, B.R. Reddy, S.K. Nash-Stevenson, Opt. Mater. 10 (1998) 225.
[30] M.Kh. Ashurov, Yu.K. Voron'ko, E.V. Zharikov, Izv. USSR Acad. Sci., Ser. Inorg. Mater. 15 (1979) 1250.